

This is the accepted manuscript made available via CHORUS. The article has been published as:

Effects of strong interactions in a half-metallic magnet: A determinant quantum Monte Carlo study

M. Jiang, W. E. Pickett, and R. T. Scalettar

Phys. Rev. B **87**, 165101 — Published 3 April 2013

DOI: [10.1103/PhysRevB.87.165101](https://doi.org/10.1103/PhysRevB.87.165101)

Effects of Strong Interactions in a Half Metallic Magnet: a Determinant Quantum Monte Carlo Study

M. Jiang^{1,2}, W.E. Pickett,¹ and R.T. Scalettar¹

¹*Physics Department, University of California, Davis, California 95616, USA and*

²*Department of Mathematics, University of California, Davis, California 95616, USA*

(Dated: March 21, 2013)

Understanding the effects of electron-electron interactions in half metallic magnets (HMs), which have band structures with one gapped spin channel and one metallic channel, poses fundamental theoretical issues as well as having importance for their potential applications. Here we use determinant quantum Monte Carlo to study the impacts of an on-site Hubbard interaction U , finite temperature, and an external (Zeeman) magnetic field on a bilayer tight-binding model which is a half-metal in the absence of interactions, by calculating the spectral density, conductivity, spin polarization of carriers, and local magnetic properties. We quantify the effect of U on the degree of thermal depolarization, and follow relative band shifts and monitor when significant gap states appear, each of which can degrade the HM character. For this model, Zeeman coupling induces, at fixed particle number, two successive transitions: compensated half-metal with spin-down band gap \rightarrow metallic ferromagnet \rightarrow saturated ferromagnetic insulator. However, over much of the more relevant parameter regime, the half-metallic properties are rather robust to U .

PACS numbers: 71.10.Fd, 71.30.+h, 02.70.Uu

I. INTRODUCTION AND BACKGROUND

As a family of promising candidates for spintronics application, half-metallic (HM) magnetic materials have attracted much interest over the past two decades^{1,2}. de Groot *et al.*³ discovered HMs computationally and popularized the HM possibility especially in Heusler and half-Heusler compounds. The distinguishing characteristic of a HM is that at the mean field level the Fermi level for one spin direction falls within a gap for the other direction, resulting in 100% polarized conduction and obvious spintronics applications. Motivated by the unusual magneto-optical properties, the Heusler class of intermetallic materials provided the most promising realizations of HM character. Thermal fluctuations degrade spin alignment and thus destroy the ideal HM. In addition, real materials effects such as crystal imperfections can couple spins and degrade the polarization; spin-orbit coupling destroys the true HM. These phenomena can be minor at low temperatures compared with the Curie temperature (which ranges 500-730 K in the half Heusler family NiMnZ (Z=Co, Pd, Pt, Sb) [4] and can be higher), but because proposed applications do not rely on 100% polarization, HMs remain viable for near-future electronic devices.

A variety of experimental techniques, including positron annihilation, spin-resolved photoemission spectroscopy, Andreev reflection, and nuclear magnetic resonance, have been employed to assess the character and polarization level of proposed HMs, often with less than definitive results. Comparison is made with density functional theory (DFT) based electronic structure calculations, which still play the dominant role in the specification of HMs and in the search for additional HMs and for the even more exotic half metallic antiferromagnets⁵⁻⁷. HMAFs, better characterized as

compensated HMs, have zero macroscopic moment so they can provide additional functionalities. Known or strongly anticipated HMs now span a diverse collection of materials with different chemical and physical properties.

An important question about HMs, not yet well clarified, is the impact of dynamic interactions (which lie beyond DFT methods) on the character and the survival of the single-spin-channel gap that defines the HM phase. One of the most fundamental consequences of repulsive on-site interactions is local moment formation and dynamics, the study of whose effects in metals has a long history (Anderson impurities, Kondo systems). Local moments in insulators are also rather well studied and present a largely distinct set of issues (gap states versus band resonances, magnetic activity)⁸. HMs, especially in oxides, bring in all of these issues: although one spin is gapped, it is not electrically an insulator since there is metallic screening, but the two spin channels are fundamentally distinct. There have now been a number of studies, in particular by Chioncel and collaborators, that indicate degradation of the HM gap – sometimes severely – by electron-electron interactions. One general picture is that interactions, typically pictured in terms of a magnetic polaron formed by charge carrier-magnon binding, lead to tailing of spectral density into the gap and sometimes to mid-gap states that would substantially degrade performance as a HM device component.

Another issue, not explicitly addressed to any great extent in treatments of interactions, is the distinction between the two types of HMs. The study of the fully polarized ferromagnet, also referred to as a saturated ferromagnet, in which the minority spin states are empty, extends back to the seminal work of Edwards and Hertz.⁹ CrO₂ is the simplest example of this: high spin $S=1$

Cr^{4+} has no occupied minority states¹⁰. The “gap” in CrO_2 is several eV wide, between occupied O $2p$ states and the unoccupied minority $3d$ bands. For low energy considerations, dc transport for example, minority spin states are out of the picture. The more common HM involves d states on either side of the gap as well as the continuum in the metallic channel; the minority charge excitations are typically narrowly gapped; in intermetallics a commonly occurring value is ~ 0.5 eV and even in oxides is rarely much greater. In the saturated case, there are simply no minority charge excitations to consider.

There have been several studies based on model Hamiltonians^{1,11–13}. In particular, work based on the s - d exchange model predicted the existence of nonquasiparticle (NQP) density of states near the Fermi level, which (mathematically) arise from the branch cut of the self-energy arising from electron-magnon interactions¹. Chioncel *et.al.* illustrated the coincidence between NQP states and the imaginary part of local spin-flip susceptibility in the framework of the single-band Hubbard Hamiltonian and DMFT approach (see below) where saturated ferromagnetism is stabilized by the additional magnetic spin splitting mimicking the local Hund rule¹¹. An effective spin Hamiltonian was derived to account for the temperature and disorder dependence of the magnetic properties of half-metallic double perovskites¹². Remarkably, Kondo screening was recently shown to stabilize ferromagnetic order and further result in a half metallic phase with minority-spin gap in the Kondo lattice model with antiferromagnetic coupling¹³.

The LDA+DMFT (local density approximation plus dynamical mean-field theory) approach that is becoming widely used to treat strong interactions is not based on a model Hamiltonian, instead using LDA results as the non-interacting system together with a self-interaction correction. This approach has been applied by Chioncel and coworkers^{11,14,15} to evaluate the effect of interactions on HMs. One of the most well studied intermetallic HMs, NiMnSb ,¹⁶ was the first application of this combined technique.¹¹ The calculated spectral density contained non-quasiparticle (NQP) states within the minority gap, but above, rather than pinned to, the Fermi level, allowing it to survive as a HM. However, further investigations of NiMnSb and other Heusler alloys show that the magnetic moment per formula unit, the NQP spectral weight, and the total DOS are insensitive or only weakly sensitive¹¹ to correlation effects. In striking contrast, correlation effects were found to play a vital role in zincblende VAs, which is calculated to be a ferromagnetic semiconductor (*i.e.* gapped in *both* spin channels) within LSDA or the generalized gradient approximation GGA, but predicted to be a half-metal ferromagnet due to band shifts produced by LSDA+DMFT.¹⁷ Strong correlation effects are also obtained in magnetite, which is uncommon in HMs in having a majority-spin gap.¹⁸ In the full Heusler

compound Mn_2VAl which is HM within LSDA,¹⁹ an LSDA+DMFT treatment of local interaction led to NQP states within the gap but below the Fermi level,¹⁵ which would not degrade spintronics-related properties. At present the impact of interactions appears to be highly material specific. However, the models and the treatment of the interactions (always approximate in some way) has varied widely, so few questions are truly settled.

The DMFT approach, which treats on-site interactions and dynamics in detail, has the shortcoming of neglecting intersite correlations. Hence spinwaves, or even short range spin order, that still contain strong correlations between neighbors, are replaced by identical but uncorrelated spin fluctuations on each interacting site. It is unclear to what degree the misrepresentation of these excitations may affect the character of the interacting spectral density.

In this paper we investigate the survival (or not) and character of HM phases based on a bilayer Hubbard model with unequal interlayer hopping for the two spin species. This model allows a substantial parameter range in which the non-interacting density of states (DOS) has a gap in only one spin channel, and will be described in detail in the next section. We note here that the layer index can be regarded equivalently as an orbital or band index, so that the bilayer Hubbard Hamiltonian provides a useful pedagogical link between single orbital and multiorbital models.

In the case when the spin up and spin down band structures are identical (*i.e.* in the absence of underlying magnetic order), tuning of the interlayer hybridization in such bilayer models has been demonstrated to drive a variety of quantum phase transitions²⁰. For example, at half filling, the ground state can have antiferromagnetic long-range order for small interlayer (interband) hopping t_\perp , and enter a disordered valence bond phase with singlet correlations between electrons on two layers, for large t_\perp . Likewise, the system can evolve through Mott insulating transitions^{21–23} as t_\perp is altered. In the doped system, there is a topological reconstruction of the Fermi surface, which modifies the spin fluctuations and changes the superconducting gap symmetry²⁴. Adopting spin-asymmetric interlayer hopping, our model introduces new avenues of behavior to be illuminated.

II. MODEL AND METHODOLOGY

A. Previous work

Previous studies of HMs in the single-band Hubbard model focused¹¹ mostly on the limiting case of saturated ferromagnetism achieved through an external Zeeman magnetic field B . With the underlying up and down spin bands being degenerate, the effective spin chemical potentials $\mu_\sigma = \mu \pm B$ are chosen to depopulate one of the species. An alternate way to achieve a half-metal, one in which the two spins species can still have the

same population so that the polarization is zero, is to alter the band structure so that a gap opens for just one of the species (which we will choose to be the “down” spins). For example, in a one band tight-binding model on a bipartite lattice with band $\epsilon(\mathbf{k})$, one can incorporate an additional staggered potential $V_{j\sigma} = (-1)^j V_\sigma$, where the $(-1)^j$ has opposite sign on the two sublattices. This alternating potential mixes momentum states \mathbf{k} and $\mathbf{k} + \pi$ and opens up a gap in the dispersion relation $E(\mathbf{k}) = \pm \sqrt{\epsilon(\mathbf{k})^2 + V_\sigma^2}$. By choosing $V_\uparrow = 0$ and $V_\downarrow \neq 0$, for an appropriate choice of Fermi level, the down spin species is insulating while the up species is metallic.

Such a staggered potential, however, couples strongly to antiferromagnetism since it provides a one body energy which favors an oscillating down spin density on the two sublattices. The dominant nature of the resulting magnetic response might obscure the determination of the effect of U on the transport properties. For example, for a half-filled square lattice Hubbard model which has a divergent antiferromagnetic susceptibility $\chi_0(\pi, \pi)$, the additional staggered potential immediately produces a state with long range antiferromagnetic order (LRAFO) which is ‘trivial’ in the sense that it does not arise from a spontaneous breaking of symmetry, but rather from the externally imposed potential. This LRAFO opens a Slater gap in the initially metallic up spin spectrum, so that U immediately, but in some sense trivially, destroys HM behavior.

B. Spin-asymmetric Hubbard model

We avoid this confusing aspect by considering instead the slightly more complex case of a two layer (or, equivalently, two orbital) square lattice Hubbard model with spin-dependent inter-layer (inter-orbital) hopping,

$$\begin{aligned} \hat{H} = & -t \sum_{\langle \mathbf{i}, \mathbf{j} \rangle m \sigma} (c_{i m \sigma}^\dagger c_{j m \sigma} + h.c.) - \sum_{i m \sigma} (\mu - \sigma B) n_{i m \sigma} \\ & - \sum_{i \sigma} t_{\perp \sigma} (c_{i 1 \sigma}^\dagger c_{i 2 \sigma} + h.c.) \\ & + U \sum_{i m} (n_{i m \uparrow} - \frac{1}{2})(n_{i m \downarrow} - \frac{1}{2}). \end{aligned} \quad (1)$$

Here the additional index $m = 1, 2$ labels two layers (orbitals) while \mathbf{i}, \mathbf{j} are site indices and σ is the spin. The first term is an intralayer nearest-neighbor hopping. We consider a square lattice with intralayer hopping $t = 1$ to set the energy scale. $t_{\perp \sigma}$ is a spin-dependent interlayer (interorbital) hybridization, and U is an on-site repulsion. The terms coupling to the density are a spin-independent chemical potential μ and a Zeeman field B . The repulsive on-site interaction term is written in particle-hole symmetric (PHS) form so that at $\mu = B = 0$ the system is half-filled (for each spin species), even if $t_{\perp \uparrow} \neq t_{\perp \downarrow}$.

The noninteracting limit $U = 0$ has two bands for each spin,

$$\begin{aligned} \epsilon_\sigma^-(\mathbf{k}) &= -t_{\perp \sigma} - 2t(\cos k_x + \cos k_y). \\ \epsilon_\sigma^+(\mathbf{k}) &= +t_{\perp \sigma} - 2t(\cos k_x + \cos k_y). \end{aligned} \quad (2)$$

For $t_{\perp \sigma} \leq 4t$ these two bands overlap, yielding metallic behavior. However, for $t_{\perp \sigma} > 4t$, Eq. 2 characterizes a band insulator with gap $2(t_{\perp \sigma} - 4t)$. Choosing one interlayer hybridization to exceed $4t$ and the other to be less than $4t$, this Hamiltonian, and choice of $U = 0$ band structure, represents a half-metal without polarization, and avoids the externally imposed antiferromagnetism which would arise from a staggered potential. The price paid is the introduction of the extra layer (orbital) degree of freedom m . The Hubbard Hamiltonian on a diamond chain is a one dimensional analog in which the interplay of perpendicular hopping and U can create a correlation-induced half metal for certain fillings²⁵.

The objective is to model interacting electrons in a ferromagnetic background of spins arising from states at higher binding energy so they do not require dynamic modeling. As has been done in previous treatments^{1,11,14,15,17}, we build in the spin symmetry breaking (ferromagnetic order) into the underlying non-interacting system. In our case it is by using a spin dependent interlayer hopping $t_{\perp \sigma}$, which is the simplest means of introducing a minority single-particle gap in this model. In DMFT calculations^{11,14,15,17} (Introduction, and Sec. IV.B) the spin asymmetry arises from the LSDA starting point and, in some of the cases, from the separate response functions arising from each spin channel. Heusler compounds, which comprise most of the material-specific treatments, provide examples²⁶ where the majority and minority bands near E_F are simply different (due for example to differing on-site energies and hoppings) rather than being Stoner-exchange split as in ferromagnetic iron.

C. Underlying magnetic order

The manner in which magnetic order (a fundamental necessity for a HM) is built into the model may affect behavior. In our model, magnetic order is implicit in the spin-dependence of $t_{\perp \sigma}$ but is otherwise unspecified. A signature aspect of our model is that for $U=0$ it is a specific realization of the schematic symmetric HMAF DOS, presented for example in Fig. 1 of Ref. [27]. In their DMFT study of a fully polarized Bethe lattice Hubbard model, Chioncel *et.al.* used a Zeeman field to mimic Hund’s rule coupling, thereby splitting the two spin directions until the minority band was empty.¹¹ In LSDA+DMFT studies of suspected HM materials (NiMnAs, FeMnSb, VAs), Chioncel and coworkers^{11,14,15} based their dynamical corrections on the spin-split LSDA bands.

The goal of this paper is to determine the effect of the electronic correlation term U in the model Hamiltonian

Eq. 1. Specifically, we compute the spin-resolved spectral densities as functions of $t_{\perp\sigma}$, U , and temperature T . We also study the interplay of U and interlayer hopping $t_{\perp\sigma}$ on the antiferromagnetic correlations. For simplicity we will set $t_{\perp\uparrow} = 0$ and vary $t_{\perp\downarrow}$ so that spin up fermions are metallic and the spin down fermions can be tuned from metal to band insulator at $t_{\perp\downarrow} = 4t$.

At the PHS point $\mu = B = 0$, both spin species are half-filled (regardless of the values of U, t, t_{\perp} or temperature T). This immediately implies the polarization is identically zero, so that our model system realizes the exotic half-metallic antiferromagnetism (HMAF)⁵. Although there has been to date no clear confirmation of novel HMAF materials, a variety of candidates have been proposed, including La_2VCuO_6 ²⁸ as a likely member of the double perovskite system with two magnetic ions,⁶ semiconductors doped with dilute magnetic ions,²⁹ and monolayer superlattices CrS/FeS and VS/CoS ³⁰. An unusual semi-Dirac half-semimetal arises in untrathin VO_2 films^{31,32}. Our model's bands closely resemble the simplest realization of a HMAF as arising from two exchange-split ions that are antialigned, shown schematically and discussed in Ref. [2]. After considering the fundamental PHS case, we will also present some results for non-zero Zeeman field B , where the system can be expected to acquire nonzero polarization.

D. DQMC procedures

We treat the interaction using the determinant quantum Monte Carlo (DQMC) technique^{33,34}. DQMC is a numerically exact approach to solve interacting tight binding electron Hamiltonians like Eq. 1. In comparison with DMFT, DQMC has the advantage of being able easily to incorporate and measure magnetic, charge, and pairing correlations between different spatial sites. On the other hand, DQMC has the drawback of being formulated on finite spatial lattices so that finite size effects must be assessed. DQMC also is limited by the fermion “sign problem”³⁵ (much more so than single site DMFT) which prevents the acquisition of data at low temperatures. Most of the results presented in this paper will be for two 8×8 layers and inverse temperatures $\beta = 6$. We will show that the sign problem is somewhat alleviated for Zeeman field $B \neq 0$ so that lower temperatures can be reached.

E. Properties to be studied

In order to distinguish metal from insulator, and see the effect of U on the half-metallicity, we will examine the single-particle density of states, $N_{\sigma}(\omega)$. This quantity is obtained by an analytic continuation of the local imaginary-time dependent Green's function $G_{\sigma}(\tau) =$

$\sum_{\mathbf{j}} \langle T c_{\mathbf{j}\sigma}(\tau) c_{\mathbf{j}\sigma}^{\dagger}(0) \rangle$, that is, by inverting,

$$G_{\sigma}(\tau) = \int_{-\infty}^{\infty} d\omega \frac{e^{-\omega\tau}}{e^{-\beta\omega} + 1} N_{\sigma}(\omega) \quad (3)$$

using the maximum entropy method³⁶. Our focus will be on the density of states at the Fermi surface $N_{\sigma}(\omega = 0)$ to see if HM behavior survives at non-zero U .

Although the system has no net polarization at $B = \mu = 0$ from the viewpoint of *total* up and down occupations, the distinction between spin directions induces a polarization of the *conduction* electrons, which is quantified by,

$$P(E_F) = \frac{N_{\uparrow}(E_F) - N_{\downarrow}(E_F)}{N_{\uparrow}(E_F) + N_{\downarrow}(E_F)} \quad (4)$$

This quantity has been the focus of much experimental work, since HMs (at $T=0$) have 100% polarization which is what makes them so attractive for spintronics applications.

We also study the dc electrical conductivity σ_{dc} , which is extracted from the current-current correlation function,

$$\Lambda_{xx}(\mathbf{k}, \tau) = \sum_{\mathbf{i}} e^{i\mathbf{k}\cdot\mathbf{l}} \langle j_x(\mathbf{l}, \tau) j_x(\mathbf{0}, 0) \rangle \quad (5)$$

where $j_x(\mathbf{l}, 0) = it \sum_{\sigma} (c_{\mathbf{l}+\mathbf{x},\sigma}^{\dagger} c_{\mathbf{l}\sigma} - c_{\mathbf{l}\sigma}^{\dagger} c_{\mathbf{l}+\mathbf{x},\sigma})$. The conductivity is obtained using the approximate form of the fluctuation-dissipation theorem^{37,38}, valid at large β ,

$$\Lambda_{xx}(\mathbf{k} = 0, \tau = \beta/2) = \pi \sigma_{dc} / \beta^2 \quad (6)$$

The magnetic structure factor

$$S(\mathbf{q}) = \frac{1}{N} \sum_{\mathbf{l}, \mathbf{j}} e^{i\mathbf{q}\cdot(\mathbf{l}-\mathbf{j})} \langle (n_{\mathbf{l}\uparrow} - n_{\mathbf{l}\downarrow})(n_{\mathbf{j}\uparrow} - n_{\mathbf{j}\downarrow}) \rangle \quad (7)$$

is of interest as well. In the ordered phase the spin correlations $\langle (n_{\mathbf{l}\uparrow} - n_{\mathbf{l}\downarrow})(n_{\mathbf{j}\uparrow} - n_{\mathbf{j}\downarrow}) \rangle$ are non-zero for large $\mathbf{l} - \mathbf{j}$ and $S(\mathbf{q})$ grows linearly with the lattice size N at the appropriate ordering wave vector \mathbf{q} .

III. CHOICE OF PARAMETER RANGES

Most HM magnets investigated to date are at most moderately correlated intermetallic compounds¹ and DFT treatments may be quite realistic. For instance, photoemission experiments and resonant x-ray scattering has led to the estimate of Hubbard interaction $U = 2$ eV for NiMnSb ³⁹, while a Wannier orbital analysis has shown that the bandwidth of the NiMnSb bands crossing E_F is $W \sim 4$ eV. The ratio $U/W \sim 1/2$ puts this HM compound in the weakly to moderately correlated regime. In our model system, the non-interacting bandwidth is $W = 8t$ at $t_{\perp} = 0$, which suggests $U/t = 0 - 4$ is the relevant range to study.

Correlation effects of this size can fundamentally change the physics of related tight-binding Hamiltonians, *e.g.* opening a correlation gap or inducing AFLRO and a Slater gap; see for example Ref. [40] and references therein. The near-neighbor square lattice tight binding model is unstable to arbitrarily small U , although this sensitivity is a result of the van Hove singularity (vHs) and perfect nesting of that model. The majority channel in our model however retains these same features (at $\mu = 0$ only, of course); in the minority channel the vHs are shifted to either side of $\mu=0$. Even with one remaining vHs, we will show below that interactions play a much less dramatic role when one spin channel is gapped.

There is, after all, new physics in a HM as well as the new phenomena discussed in Sec. I: the new energy scale that is given by the spin-down gap $\Delta = 2(t_{\perp,\downarrow} - 4t)$. Down-spin charge excitations are gapped by Δ , which make interactions further differentiate the spins, for example by enabling sharp ‘impurity’ states (only) within the spin-down gap. Spin-flip interactions are gapped by the separation between μ (the up-spin Fermi level) and the nearest down-spin band edge, which is $\Delta/2$ at $\mu=0$ in our model. Kondo processes vanish due to the absence of low energy spin-flip excitations. Perhaps more relevantly, the vHs- and nesting-driven spin density wave instability obviously will be quenched when there is a minority gap. We show it is also suppressed in the ferromagnetic metal phase where the minority bands are split but not gapped.

IV. EFFECT OF ON-SITE INTERACTION

A. DQMC results

The moderating of strong interaction effects is seen in the density of states, shown in Fig. 1, where the insulating species $N(\omega)$ at $U/t = 4$ is virtually indistinguishable from its $U = 0$ form. Here we have set $t_{\perp\uparrow} = 0$ and $t_{\perp\downarrow} = 5t$ and $\mu = B = 0$ so that the down spin species has a noninteracting band gap $\Delta = 2(t_{\perp\downarrow} - 4t) = 2t$ and the up species is metallic. The gap magnitude and tailing of states into the gap is unaltered up to $U=4$. The up (metallic) species $N_{\uparrow}(E_F)$ is also constant from $U/t = 0$ to $U/t = 4$ to within the accuracy of the maximum entropy inversion of Eq. 3. The peaks in $N_{\uparrow}(\omega)$ away from $\omega = 0$ are affected by the finite size effect of the 8×8 lattice.

One distinguishing characteristic of interactions in HMs extensively discussed in previous studies is the appearance of the non-quasiparticle (NQP) states within the spectral gap – the magnetic polaron effect. These NQP states in previous studies have (1) appeared, at $\omega = 0$, above $\omega = 0$, and below $\omega = 0$, and (2) also possibly not appeared. In the generic picture, the density of NQP states vanishes at the Fermi level ($\omega = 0$) but increases toward an energy scale of the order of the magnon frequency, leading to an asymmetry of spectral function.¹

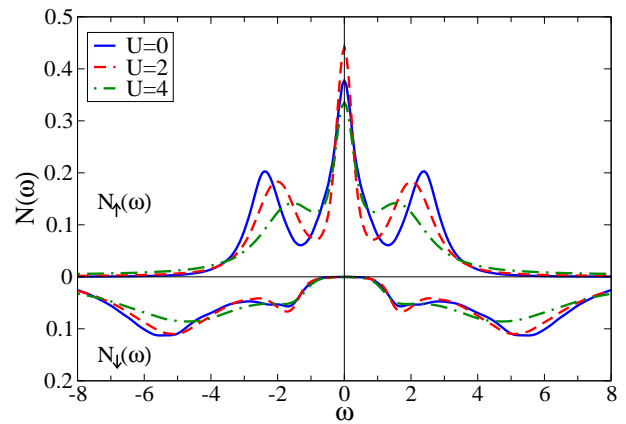


FIG. 1: Half metallic behavior persists in the presence of interactions: the down species density of states is virtually unaltered at $U/t = 4$ from its $U/t = 0$ value. Here $t_{\perp\uparrow} = 0$ and $t_{\perp\downarrow} = 5$ so that the down species (only) has a noninteracting band gap $\Delta = 2t$. The up species is metallic with a density of states at the Fermi surface that is relatively insensitive to U . The lattice size $N = 8 \times 8$ in each layer and the inverse temperature $\beta = 5$. The chemical potential and Zeeman fields $\mu = B = 0$. However, due to the particle-hole symmetry at half filling, there is no signature associated with the NQP states.

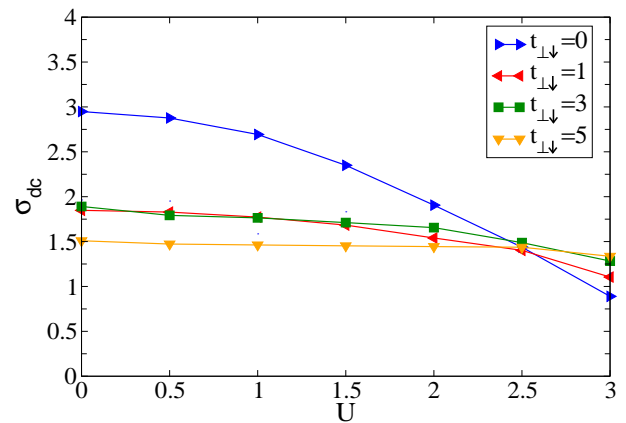


FIG. 2: The dc conductivity for $\beta = 6$ is shown as a function of U . For the half metal $t_{\perp\downarrow} = 5t$, U has very little effect on σ_{dc} , which is consistent with the invariance of the density of states in Fig. 1. In a fully metallic phase $t_{\perp\downarrow} = 0$ there is a clear decrease of σ_{dc} with U due to the additional electron-electron scattering which can occur when both species have nonzero density of states at the Fermi surface.

Assisted perhaps by the particle-hole symmetry in our model (implying the symmetry of spectral function) at half filling, NQP states may be inhibited from appearing, and there is no signature of NQP states in Fig. 1. The implicit nature of magnetic order in our model may also play a role, but other treatments have also incorporated some implicit origin of the magnetic order in a HM.

The HM character can be expected to become more or less evident in a property specific manner, and we now

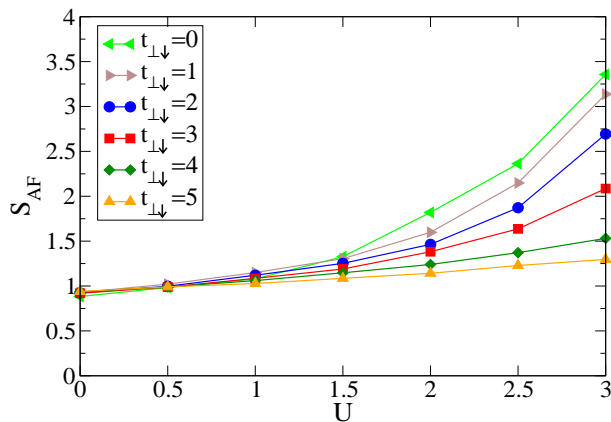


FIG. 3: Staggered static structure factor S_{AF} through the metal-HM transition. Increasing interlayer coupling reduces the increase with increasing U until, for half metallic phase $t_{\perp\downarrow} = 5$, U has little effect on the (small) magnetic coupling. In symmetric bilayers, large interlayer promote singlet formation, which are suppressed here by the HM gap.

describe a few examples. The relatively minor effect of on-site interaction U is further evidenced by the behavior of the dc-conductivity in Fig. 2, where the interlayer coupling is varied to move the system through the metallic phase $t_{\perp\downarrow}=2, 3$, through the transition $t_{\perp\downarrow}=4$, to the HM phase $t_{\perp\downarrow}=5$. At $t_{\perp\downarrow}=2$ the conductivity is U -dependent because $N(\omega \rightarrow 0)$ in the metallic phase has the underlying van Hove singularity there. As U increases the $t_{\perp\downarrow}$ dependence weakens, and at $t_{\perp\downarrow}=4$ and 5, which is crossing over into the HM phase, σ_{dc} decreases and becomes independent of the interaction strength: in the HM phase $t_{\perp\downarrow} = 5$, σ_{dc} falls by less than ten percent as U increases from $U = 1$ to $U = 3$, and must be controlled solely by spin-up processes.

Fig. 3 demonstrates the correlation effects on the staggered magnetic static structure factor, again for the progression from metal to HM $t_{\perp\downarrow}=2-5$. The increase with U at small interlayer coupling decreases as the HM phase is approached and entered, and the variation of S_{AF} with U in the HM phase $t_{\perp\downarrow} = 5$ is quite small. It is unlikely that antiferromagnetic long-range order will arise at lower temperatures, and it is known that, in the case of spin-independent interlayer hybridization, t_{\perp} drives a competing singlet ground state, with a quantum critical point at $t_{\perp} \sim 1.6$ above which the ground state of the bilayer model no longer has AFLRO in its ground state.

B. Relation to Previous Work

To illustrate the similarity (or difference) of our results to previous work, it is instructive to describe, in brief fashion, most of the former results for interacting half metals with different model usage and theoretical approaches in terms of the existence (or not) of NQP

states.

As previously noted, in early work Chioncel and coworkers¹¹ studied within DMFT the Hubbard model with an imposed exchange splitting on a Bethe lattice (BL). They obtained a split-off peak in the spectral density at high energy, and the BL spectra in both spin channels assume a two peak structure. The low lying minority states, centered 0.5 eV above but slightly overlapping E_F , were identified as NQP states. They then applied LDA+DMFT to the FM LDA state for NiMnSb including a Hubbard interaction on Mn and a spin-asymmetric T-matrix fluctuation exchange (TMFX) approach. In addition to other spectral changes, they obtained NQP states just above Fermi level. A variational cluster approximation treatment (a cluster DMFT method) for NiMnSb has also been reported⁴⁴, to begin to assess the influence of interatomic correlation on the HM state. The main features of the spectra were not altered greatly from the earlier results.

A study of HM Heusler compounds, based on the LSDA FM state and including a Hubbard interaction treated within LDA+DMFT obtained a small NQP peak in the spectral density of half-Heusler FeMnSb falling at E_F for $U = 4$ eV but a clean gap for $U=2$ eV (as for LSDA, $U=0$). Following this discovery of dependence of NQP states on model parameters, a study to identify appropriate parameters was reported by Yamasaki *et al.*⁴¹ Calculations⁴² for Co_2MnSi , again using the TMFX method to treat the DMFT atomic problem, led to the Fermi level above a clean minority gap, E_F almost coinciding with the top of the minority gap, varying somewhat with temperature. One effect of the interactions can be characterized as a shift downward of minority states by 0.1 eV with respect to LSDA. Unlike most HM Heusler compounds, Mn_2VAl displays its gap in the majority channel. An LDA+DMFT(TMFX) treatment of this compound⁴³ led to NQP states below the gap, and the positioning of the Fermi level switched from the top of the gap (LSDA) to the bottom (DMFT) due to interactions and the interaction-induced changes in self-energy. As discussed in somewhat more detail later, the position of the Fermi level with respect to the gap involves an issue, perhaps delicate, of band filling.

Results have also been presented for HM CrO_2 , both within LDA+DMFT (downfolded to t_{2g} orbitals) and within VCA (virtual crystal approximation)⁴⁵, each method involving somewhat different approximations and treatments of interactions. The minority spin persisted, but the gap was reduced by NQP contributions to the spectral density until the Fermi level coincided with the top of the minority gap. This positioning of the Fermi level is exactly that in which the spin gap (within these treatments) vanishes. The NQP states are not pinned to the Fermi level, but about it.

Our model and method reveals no obvious NQP states, certainly not within the gap and near the Fermi level. In our studies of spectra, we have kept the chemical potential at the center of the gap, thus well removed

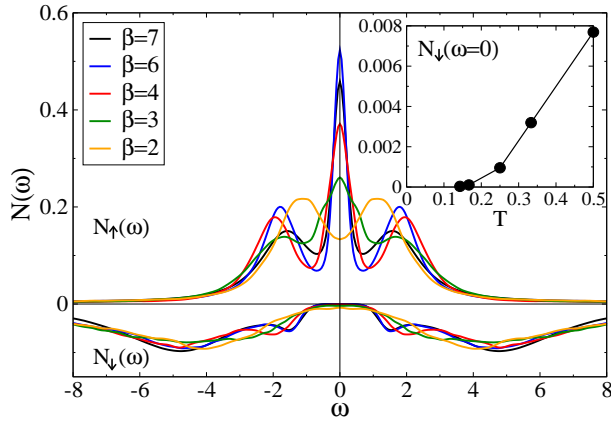


FIG. 4: Main panel: Temperature effects on the density of states of half-metallic phase ($U = 3$). The inset shows $N_{\downarrow}(\omega = 0)$ versus T . The half-metal gap in $N_{\downarrow}(\omega)$ appears to be robust for $\beta > 3$ ($T < t/3$).

from the minority band edges, and this may affect the appearance and strength of NQP states. It is also difficult to make a real comparison of a model with two non-collocated s -like orbitals with the multiorbital d compounds. The interaction is however treated without approximation, and the finite lattice builds in interatomic correlations and thereby includes a representation of q -dependent magnon-like excitations and self-energy.

Despite the fact that DQMC treats interactions exactly, the model of Eq. 1 does not explicitly retain Hund's rule terms (an approximation in common with most QMC work). An open issue, in both our work and in the DMFT treatments, is the accuracy of the representation of spin flip processes which have been identified⁴⁶ as responsible for the NQP states. The non-interacting single particle gap in Eq.1 precludes the presence of low lying magnon excitations which are present, for example, in spin-symmetric bilayer and multi-orbital models which have long range antiferromagnetic order and hence no spin gap at small intersheet coupling^{47,48}.

V. EFFECT OF TEMPERATURE

The temperature dependence of the half-metallic properties and their stability against finite-temperature spin excitations are crucial for practical applications. As mentioned before, one crucial effect is the depolarization caused by finite-temperature. With the separate spin bands fixed in our model, the effect of reduced magnetization upon approaching the Curie temperature is not included, but we can study temperature effects “at fixed magnetization.”

Fig. 4 illustrates the temperature effects on the density of states in the half-metallic phase. While substantial rearrangements of spectral weight occur for spin up, the primary effect for spin down is an increased tailing of

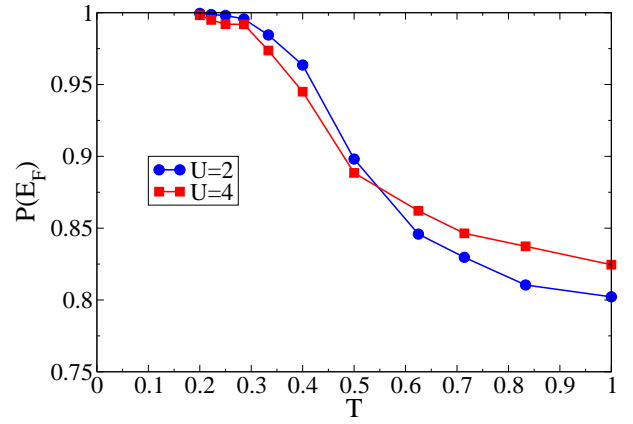


FIG. 5: The temperature dependence of the conduction electron spin polarization, where the non-interacting gap is equal to $\Delta = 2t$ ($t=1$). $P(E_F)$ begins to turn downwards at $T \sim \Delta/6$, with minor dependence on the value of U .

states across the band edges and into the gap as T increases. Only when $\beta < 3$ is the half-metallic feature destroyed, *i.e.* $N_{\downarrow}(\omega \rightarrow 0)$ becomes appreciably non-zero. This corresponds to a temperature $T \sim t/3 \sim \Delta/6$ since the down spin band gap $\Delta = 2t$. If we phenomenologically introduce $\Delta(T)$ which vanishes at the Curie temperature, and suppose that the magnitude of the gap is the primary energy scale for this purpose, then we can infer destruction of HM character by interactions (and thermal broadening) around $T^* = \Delta(T^*)/6$.

We can also examine thermal effects by evaluating the conduction electron spin polarization $P(E_F)$. The combined effects of finite-temperature and Hubbard interaction U are given in Fig. 5. The polarization begins to deviate downwards from unity at $T \sim t/3$. The role of U on $P(E_F)$ is negligible in the low temperature regime, but as T increases to intermediate temperatures U has a distinct depolarization effect. Thinking of our parameters as very roughly relevant to NiMnSb, $t/3$ is a very high temperature, one at which the underlying magnetic order (fixed in our model) physically has diminished drastically or vanished. Even well above room temperature thermal effects as well as effects due to interaction U up to 4 on $P(E_F)$ are negligible.

A separate diagnostic of the nature of half-metallic phase and its robustness against the Hubbard interaction U is provided by the conductivity, Fig. 6, evaluated from Eq. 6. Recall that in a half metal for these values of parameters, the conductivity arises only from the majority (ungapped) channel, and spin-flip scattering is frozen out at these temperatures leaving scattering only in the charge channel. This data supports the previous indications of the relatively small effects of interactions in our bilayer model of a half metal. The primary difference for $U = 2$ is the significantly larger conductivity when T falls below $0.2t$, compared to the $U = 4$ trajectory. On the other hand, σ_{dc} at higher temperatures hardly

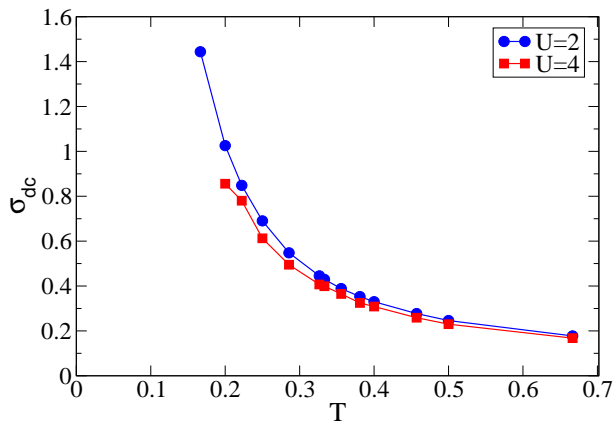


FIG. 6: Temperature dependence of conductivity, for $U=2$ and 4. In the HM phase ($t_{\perp\downarrow} = 5$) the conductivity (see Eq. 6) is contributed only by the up spin carriers, which as noted earlier is not affected strongly by these values of U .

depends on U .

VI. EFFECT OF ZEEMAN MAGNETIC FIELD

All of results above are at $\mu = B = 0$ which, by particle-hole symmetry, guarantees half filling of both spin species: $\langle n_{i\mu\sigma} \rangle = 0.5$. A Zeeman field B introduces a spin bias, but one of the signatures of a HM is that it is impervious to magnetic fields that are not too large, that is, as long as the gap persists and μ does not cross a gap edge. This vanishing of the spin susceptibility is self-evident at the mean field level, where B merely shifts the relative positions of the up and down bands. If the chemical potential (finally determined by state filling in the metallic channel) does not cross either gap edge, there is no reoccupation of states of either spin. In fact there is no change (up to a constant) in the real-space potential for either spin, so the (many-body) states themselves do not change. The energy changes only due to the trivial magnetic energy term $-MB$ (M is the net magnetization, which is unchanging until μ crosses a band edge) which is zero in our HMAF-type model.

The interest here is in interacting systems, and this anticipated behavior of HMs has been supported by some rigorous results based on ground state many-body wavefunctions and spin density functional theory^{49,50}. The theory provides for ranges of applied Zeeman fields for which the ground state, and therefore the spin-density matrix is unchanging, just as at the mean field level. The values of the applied fields, positive and negative, at which the magnetism changes thereby provides the gap edges, and their difference provides the (interacting) fixed particle number gap.

In our calculations when $t_{\perp\uparrow} = t_{\perp\downarrow}$ and $B = \mu = 0$ there is no sign problem at any temperature. This is a consequence of a total correlation between the signs of the up and down spin determinants, so that their

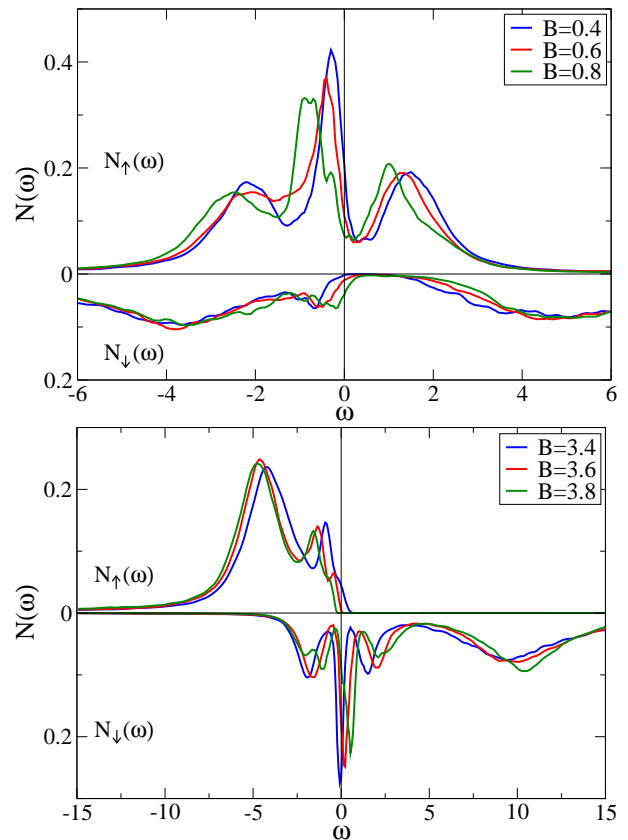


FIG. 7: Effects of Zeeman field B on the density of states, at fixed μ . Here $U = 3, \beta = 8, t_{\perp\downarrow} = 5$. The Zeeman field B shifts the spectral function of both spin species. Top panel: At weak fields (viz. less than half the gap), $N(\omega)$ more or less rigidly shifts with B for both spin species, as in mean field. In the case of the insulating down spin electrons this shift eliminates insulating behavior as B approaches half the band gap $2(t_{\perp} - 4t)$ and the magnetization begins to change. Bottom panel: At large magnetic field the up spin density of states is driven completely below the Fermi level $\mu + B$ so that now the up species is insulating. Meanwhile the down spin density is metallic because, with its larger bandwidth, the down spin Fermi level $\mu - B$ is not yet completely below the down bands. In this way one has a HM in which the metal/insulator roles of the two spin species is reversed.

product, the probability of the configuration, is always positive. Allowing μ or B to become nonzero induces a sign problem so that, normally, simulations are much more challenging. Here, however, with $t_{\perp\uparrow} \neq t_{\perp\downarrow}$ the correlation between spin up and spin down determinants has already been broken, which is why our simulations in the earlier sections do not extend beyond $\beta \approx 6$. We can access a similar range here when $B \neq 0$.

In mean-field level, the effect of the external Zeeman field is only to shift the spectral functions of both spin species rigidly in opposite directions. It is therefore natural to expect a transition from half-metallic phase to normal phase at $|B_c|$ equal to half the band gap. We show that this transition survives in the presence

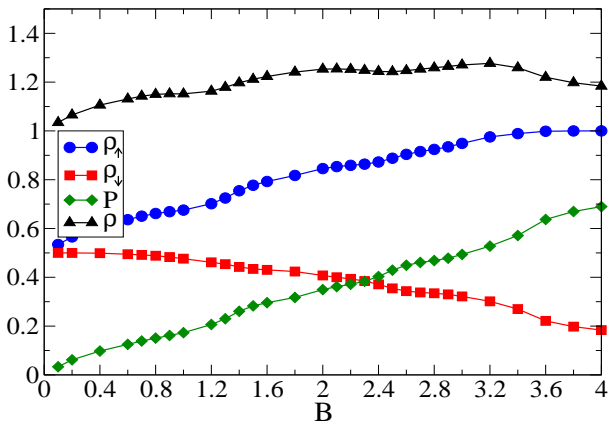


FIG. 8: Up, down, and total density as function of Zeeman field at fixed $\mu = 0$ and increasing B . The system starts at half-filling $\rho_{\uparrow} = \rho_{\downarrow} = 0.5$ at $B = 0$ and becomes increasingly spin polarized as B increases. Ultimately at $B \sim 4$ equal to half the band-width, the up bands are completely filled. This value of B is not quite sufficient to empty the down band owing to its slightly larger band-width. The polarization is $P = (\rho_{\uparrow} - \rho_{\downarrow})/(\rho_{\uparrow} + \rho_{\downarrow})$. The parameters are chosen as $U = 3, \beta = 8$.

of Hubbard interaction U , but with spectral weight redistribution which is not captured in MF in addition to renormalization of B_c .

Fig. 7 shows the effects of Zeeman field on the spectral density. In the top panel the weak magnetic field-induced shifting of the spectral weights of both spin species in the opposite directions is clear, though the shifts begin to deviate from being rigid. HM character survives to $B_c \approx 0.4$, compared to $B_c = 0.5$ without interactions. This “magnetic field gap” is renormalized by $\sim 20\%$ at $U=3$. In the bottom panel, we demonstrate that a strong enough magnetic field (of order the half the bandwidth, $B \sim W/2$) can induce a situation in which the up spin electron bands become completely filled (heuristically, the effective chemical potential $\mu_{\text{eff}\uparrow} = \mu + B$ lies above the band), while the down spin electrons remain metallic: $\mu_{\text{eff}\downarrow} = -\mu + B$ still cuts across a region of nonzero $N_{\downarrow}(\omega)$. Since the filled majority channel holds one electron, the occupation of some minority states reflects the fact that the total density has increased as the field is increased at fixed chemical potential $\mu=0$. At fixed particle density, a large field will indeed produce a filled majority band, in which the minority band must be empty (the non-zero spectral density must lie only above $\mu=0$). This state is a saturated ferromagnetic insulator. In this way, as B increases, the sequence of phases at fixed μ proceed from HM with majority carriers \rightarrow metallic ferromagnet \rightarrow HM with minority carriers. This sequence converts, at fixed density, to HM with majority carriers \rightarrow metallic ferromagnet \rightarrow saturated ferromagnet insulator.

Another reflection of the magnetic behavior, again at fixed $\mu=0$, is illustrated in Fig. 8. The external Zeeman magnetic field leads to an increasingly polarized

lattice [top panel, $P = (\rho_{\uparrow} - \rho_{\downarrow})/(\rho_{\uparrow} + \rho_{\downarrow})$], as ρ_{\uparrow} grows monotonically at the expense of ρ_{\downarrow} . At $B \sim 4$ the up bands are completely full while the down bands, which due to their nonzero $t_{\perp\downarrow}$ have a larger bandwidth, are still crossed by the effective chemical potential. This appears to be re-entry into a (polarized) HM phase. However, the spectra in Fig. 7 and the data of Fig. 8 were obtained at constant μ , and the B-induced increase in density has been recognized but does not affect this picture.

VII. SUMMARY

We have used the numerically exact finite-temperature determinant Quantum Monte Carlo (DQMC) method to study the effect of strong interaction induced correlations on half-metallic behavior in a multiband Hubbard Hamiltonian. Our model consists of a bilayer square lattice, or, alternately viewed, a two orbital system, with spin-dependent interlayer hybridization chosen to induce a band gap in only one spin species. This is a model appropriate to half metallic antiferromagnets, since the lattice has the same number of spin up and spin down electrons, but only the latter have a gapped non-interacting spectrum.

By investigating the influence of an on-site Hubbard interaction U , finite temperature T and external Zeeman magnetic field B , we find that the half-metallic properties are not particularly sensitive to the interaction U , up to values equal to about half the bandwidth which seem appropriate to intermetallic half metals. Finite-temperature effects depolarize the conduction electron states only at $T > t/3$ of the gap, with a degree of depolarization which depends weakly on U . A very large Zeeman magnetic field drives the system (at fixed particle number) from half metal to metallic ferromagnet, and finally to a ferromagnetic insulating phase when the minority spectral density is Zeeman split completely above the majority spectrum.

An interesting issue in half-metallic ferromagnetic materials that remains undecided is when non-quasiparticle (NQP) states arising from electron-magnon interaction arise, and whether they are above, below, or spanning the chemical potential. The signature of such states is the appearance of a resonance in the gapped channel. In contrast to several earlier studies based on different models and using a different treatment of the interaction, we have not seen any distinct characteristic features associated with NQP states in the DQMC studies of our model. The difference may be related to the fact that our bilayer system without the external magnetic field satisfies particle-hole symmetry so that E_f is always pinned to the center of the gap. Spin-flip processes become more accessible as the chemical potential approaches a gap edge. The other possibility is that the sign problem has prevented us from reaching low enough temperature to observe the development of the resonance, or that the spin waves that may be required

for a proper description of electron-magnon interactions are not yet fully formed. It is possible that the effects of interactions are simply model and material dependent rather than universal.

VIII. ACKNOWLEDGEMENTS

We thank R.H.C. Peppers for useful input, and acknowledge informative communication with L. Chioncel and M. I. Katsnelson. M.J. was supported by the National Science Foundation under grant PHY-1005503, and R.T.S. and W.E.P. received support from the Department of Energy Stewardship Science Academic Alliances Program DE-NA0001842.

- ¹ M.I. Katsnelson, V.Y. Irkhin, L. Chioncel, and R.A. de Groot, *Rev. Mod. Phys.* **80**, 315 (2008).
- ² W.E. Pickett and J.S. Moodera, *Physics Today*, May 2001, page 39.
- ³ R. A. de Groot, F. M. Mueller, P. G. van Engen and K. H. J. Buschow, *Phys. Rev. Lett.* **50**, 2024 (1983).
- ⁴ P. J. Webster and K. R. A. Ziebeck, *Alloys and Compounds of d-elements with main group elements*, part 2, Landolt-Boörnstein, New Series, Group III, Vol. 19c, edited by H. R. J. Wijn, Springer-Verlag, Berlin (2001), pp. 75-184.
- ⁵ R.A. de Groot, *Physica B*, **172**, 45 (1991); H. van Leuken, R.A. de Groot, *Phys. Rev. Lett.* **74**, 1171 (1995).
- ⁶ W.E. Pickett, *Phys. Rev. Lett.* **77**, 3185 (1996); W.E. Pickett, *Phys. Rev. B* **57**, 10613 (1998).
- ⁷ X. Hu, *Adv. Mater.* **24**, 294 (2012).
- ⁸ *Lecture Notes on Electron Correlation and Magnetism*, P. Fazekas (World Scientific, Singapore, 1999).
- ⁹ D. M. Edwards and J. A. Hertz, *J. Phys.: Metal Phys.* **3**, 2191 (1973).
- ¹⁰ D.J. Huang,, L.H. Tjeng, J. Chen, C.F. Chang, W.P. Wu, S.C. Chung, A. Tanaka, G.Y. Guo, H.J. Lin, S.G. Shyu, C.C. Wu, and C.T. Chen, *Phys. Rev. B* **67**, 214419 (2003).
- ¹¹ L. Chioncel, M.I. Katsnelson, R.A. de Groot, and A.I. Lichtenstein, *Phys. Rev. B* **68**, 144425 (2003).
- ¹² O. Erten, O.N. Meetei, A. Mukherjee, M. Randeria, N. Trivedi, and P. Woodward, *Phys. Rev. Lett.* **107**, 257201 (2011).
- ¹³ R. Peters, N. Kawakami, and T. Pruschke, *Phys. Rev. Lett.* **108**, 086402 (2012).
- ¹⁴ L. Chioncel, M.I. Katsnelson, G.A. de Wijs, R.A. de Groot, and A.I. Lichtenstein, *Phys. Rev. B* **71**, 085111 (2005).
- ¹⁵ L. Chioncel, E. Arrigoni, M.I. Katsnelson, and A.I. Lichtenstein, *Phys. Rev. Lett.* **96**, 137203 (2006).
- ¹⁶ K.E.H.M. Hanssen, P.E. Mijnders, L.P.L.M. Rabou, and K.H.J. Buschow, *Phys. Rev. B* **42**, 1533 (1990).
- ¹⁷ L. Chioncel, P. Mavropoulos, M. Lezaic, S. Blügel, E. Arrigoni, M.I. Katsnelson, and A.I. Lichtenstein, *Phys. Rev. Lett.* **96**, 197203 (2006).
- ¹⁸ L. Craco, M.S. Laad, and E. Muller-Hartmann, *Phys. Rev. B* **74**, 064425 (2006); I. Leonov, A.N. Yaresko, V.N. Antonov, and V.I. Anisimov, *Phys. Rev. B* **74**, 165117 (2006).
- ¹⁹ R. Weht and W. E. Pickett, *Phys. Rev. B* **60**, 13006 (1999).
- ²⁰ R.E. Hetzel, W. Linden, and W. Hanke, *Phys. Rev. B* **50**, 4159 (1994); and R.T. Scalettar, J.W. Cannon, D.J. Scalapino, and R.L. Sugar, *Phys. Rev. B* **50**, 13 419 (1994).
- ²¹ A. Liebsch, *Phys. Rev. B* **70**, 165103 (2004).
- ²² R. Arita and K. Held, *Phys. Rev. B* **72**, 201102(R) (2005).
- ²³ M. Sentef, J. Kuneš, P. Werner and A. P. Kampf, *Phys. Rev. B* **80**, 155116 (2009).
- ²⁴ D.J. Scalapino, *Rev. Mod. Phys.* **84**, 1383 (2012); N. Bulut, D.J. Scalapino, and R.T. Scalettar, *Phys. Rev. B* **45**, 5577 (1992).
- ²⁵ Z. Gulacsi, A. Kampf, and D. Vollhardt, *Phys. Rev. Lett.* **99**, 026404 (2007).
- ²⁶ I. Galanakis, P. H. Dederichs, and N. Papanikolaou, *Phys. Rev. B* **66**, 134428 (2002).
- ²⁷ R. E. Rudd and W. E. Pickett, *Phys. Rev. B* **57**, 557 (1998).
- ²⁸ V. Pardo and W. E. Pickett, *Phys. Rev. B* **84**, 115134 (2011).
- ²⁹ K. Sato, H. Katayama-Yoshida, and P. H. Dederichs, *J. Supercond.* **16**, 31 (2003).
- ³⁰ M. Nakao, *Phys. Rev. B* **77**, 134414 (2008).
- ³¹ V. Pardo and W. E. Pickett, *Phys. Rev. Lett.* **102**, 166803 (2009).
- ³² S. Banerjee, R. R. P. Singh, V. Pardo, and W. E. Pickett, *Phys. Rev. Lett.* **103**, 016402 (2009).
- ³³ R. Blankenbecler, D.J. Scalapino, and R.L. Sugar, *Phys. Rev. D* **24**, 2278 (1981).
- ³⁴ S.R. White, D.J. Scalapino, R.L. Sugar, E.Y. Loh, Jr., J.E. Gubernatis, and R.T. Scalettar, *Phys. Rev. B* **40**, 506 (1989).
- ³⁵ E.Y. Loh, J.E. Gubernatis, R.T. Scalettar, S.R. White, D.J. Scalapino, and R.L. Sugar, *Phys. Rev. B* **41**, 9301 (1990).
- ³⁶ J.E. Gubernatis, M. Jarrell, R.N. Silver, and D.S. Sivia, *Phys. Rev. B* **44**, 6011 (1991). We use a code written by Fakher Assaad.
- ³⁷ M. Randeria, N. Trivedi, A. Moreo, and R. T. Scalettar, *Phys. Rev. Lett.* **69**, 2001 (1992); N. Trivedi and M. Randeria, *ibid.* **75**, 312 (1995).
- ³⁸ Use of this expression avoids the necessity of the analytic continuation of the current-current correlation functions. However, it also involves the assumption that the temperature is much less than the energy scale Ω at which $\text{Im}\Lambda$ deviates from its low frequency behavior $\text{Im}\Lambda \sim \omega\sigma_{dc}$. This may not be valid for systems in which there is no randomness, e.g. for a Fermi liquid $\Omega \sim 1/\tau_{el-el} \sim N(0)T^2$ so that the validity condition is never satisfied. See N. Trivedi, R.T. Scalettar, and M. Randeria, *Phys. Rev. B* **54**, 3756 (1996).
- ³⁹ E. Kisker, C. Carbone, C.F. Flipse, and E.F. Wassermann, *J. Magn. Magn. Mater.* **70**, 21 (1987); M. V. Yablonskikh, Y.M. Yarmoshenko, V.I. Grebennikov, E.Z. Kurmaev, S.M. Butorin, L.C. Duda, J. Nordgren, S. Plogmann, and M. Neumann, *Phys. Rev. B* **63**, 235117 (2001).
- ⁴⁰ D. Vollhardt, *Ann. Phys. (Berlin)* **524**, 1 (2012). DOI 10.1002/andp.201100250.
- ⁴¹ A. Yamasaki, L. Chioncel, A. I. Lichtenstein, and O. K. Andersen, *Phys. Rev. B* **74**, 024419 (2006).
- ⁴² L. Chioncel, Y. Sakuraba, E. Arrigoni, M. I. Katsnelson, M. Oogane, Y. Ando, T. Miyazaki, E. Burzo, and A. I. Lichtenstein, *Phys. Rev. Lett.* **100**, 086402 (2008).
- ⁴³ L. Chioncel, E. Arrigoni, M. I. Katsnelson, and A. I. Lichtenstein, *Phys. Rev. B* **79**, 125123 (2009).
- ⁴⁴ H. Allmaier, L. Chioncel, E. Arrigoni, M. I. Katsnelson, and A. I. Lichtenstein, *Phys. Rev. B* **81**, 0554422 (2010).
- ⁴⁵ L. Chioncel, H. Allmaier, E. Arrigoni, A. Yamasaki, M. Daghofer, M. I. Katsnelson, and A. I. Lichtenstein, *Phys. Rev. B* **75**, 140406(R) (2007).
- ⁴⁶ V.Y. Irkhin and M.I. Katsnelson, *J. Phys.: Condens. Matter*, **2**, 7151 (1990).
- ⁴⁷ R.T. Scalettar, J.W. Cannon, D.J. Scalapino, and R.L. Sugar, *Phys. Rev. B* **50**, 13419 (1994).
- ⁴⁸ M. Vekic, J.W. Cannon, D.J. Scalapino, R.T. Scalettar, and R.L. Sugar, *Phys. Rev. Lett.* **74**, 2367 (1995).
- ⁴⁹ H. Eschrig and W. E. Pickett, *Solid State Commun.* **118**, 123 (2001).
- ⁵⁰ K. Capelle and G. Vignale, *Phys. Rev. Lett.* **86**, 5546 (2001).